inset of Fig. 4a). A saturation magnetization of 6 emu g^{-1} (1 emu g^{-1} = 1 A m^2 kg^{-1}) is achieved with an applied field of 8000 Oe (1 Oe = 10^{-4} T). The remnant magnetization and coercivity are 4 emu g^{-1} and 2000 Oe, respectively. The magnetic susceptibility of the $Fe_{1-x}S$ (x = 0.08–0.1) nanowires, **III**, on the other hand, is different from that of **II**. Nanowires of **III** show a lambda-type transition[10] at 420 K in the high-temperature susceptibility data (Fig. 4b). Except in the narrow temperature range of 375–475 K, the ferrimagnetism disappears on either side and predominant antiferromagnetism becomes evident. The antiferromagnetic to paramagnetic transition occurs at 600 K. On cooling the sample, the peak disappears showing a Weiss-type behavior, a mixed behavior common in the $Fe_{1-x}S$ phases.[9] **III** does not exhibit a hysteresis loop at room temperature and the magnetization is at least one order of magnitude smaller than that of **II**, indicating predominant antiferromagnetic interactions. We must point out that the magnetic properties reported here represent the average behavior of a bundle of nanowires. It has not been possible to strictly compare the observed properties with those of the bulk, since the literature reports on the bulk properties vary rather widely. Electrical resistivity measurements on pressed pellets of Fe_7S_8 and $Fe_{1-x}S$ nanowires show semiconducting behavior at room temperature and below.

In conclusion, we have been successful in developing a one-step synthesis to produce iron sulfide nanowires of well-defined compositions in high yields. The isolation and characterization of magnetic Fe_7S_8 nanowires are noteworthy.

Experimental

The synthesis procedure of $Fe_{1-x}S$ nanowires comprises two steps. In the first step, solvothermal methods have been employed to obtain an organic–inorganic composite (**I**), $Fe_{1-x}S(en)_{0.5}$. The amine removal from this composite by heating under a flow of Ar at 200–300 °C yielded nanowires of $Fe_{1-x}S$.

*Preparation of the Organic–Inorganic Composite, **I***: In a typical synthesis procedure, $FeCl_2{\cdot}4H_2O$ (0.2982 g, 1.5 mmol) was mixed with CH_3CSNH_2 (thioacetamide, 0.2254 g, 3 mmol) in a Teflon-lined steel autoclave (23 ml capacity) and 10 mL ethylenediamine was added to it. The container was sealed and heated to 180 °C for 4 days under solvothermal conditions. A purple-blackish wool-like flocculate was obtained, which was immediately sonicated in methanol, filtered, washed with methanol, and dried in vacuum. It should be noted that the as-synthesized product is always stored under vacuum as longer exposure to air under ambient conditions leads to conversion of the iron-sulfide phases to the oxide/hydroxide phases. For this reason, after opening the autoclave, sonication and filtration were carried out in minimum time.

*Synthesis of Fe_7S_8 (**II**) and $Fe_{1-x}S$ (**III**) Nanowires by Amine Removal from the Composite **I***: The composite **I** was taken in a quartz boat and placed inside a quartz tube, which was put in a horizontal tubular furnace. The sample was heated under a flow of Ar (200 sccm) to 200–300 °C and kept at that temperature for 20–30 min. The furnace temperature was allowed to come down to room temperature naturally before taking out the product. The color of the reactant powder changed to black after the thermal treatment. Fe_7S_8 nanowires (**II**) were obtained at 200 °C, while at 300 °C, $Fe_{1-x}S$ (x = 0.08–0.1) nanowires (**III**) were produced.

Characterization: The samples were characterized by powder XRD (Seifert 3000TT), SEM (Leica S440i fitted with Leo software for EDX analysis), TEM (JEOL JEM 3010, operating at 300 kV), IR spectroscopy (Bruker *IFS*-66v/S). Magnetic measurements were carried out using a VSM (LakeShore) and by the Faraday technique (Lewis Coil force magnetometer, George Associates).

Received: August 19, 2003
Final version: October 4, 2003

[1] a) J. Hu, T. Wang Odom, C. M. Leiber, *Acc. Chem. Res.* **1999**, *32*, 435. b) Y. Xia, P. Yang, Y. Sun, Y. Wu, B. Mayers, B. Gates, Y. Yin. F. Kim, H.Yan, *Adv. Mater.* **2003**, *15*, 353.
[2] a) T. Thurn-Albrecht, J. Schotter, G. A. Kästle, N. Emley, T. Shibauchi, L. Krusin-Elbaum, K. Guarini, C. T. Black, M. T. Touminen, T. P. Russell, *Science* **2000**, *290*, 2126. b) J. Bao, C. Tie, Z. Xu, Q. Zhou, D. Shen, Q. Ma, *Adv. Mater.* **2001**, *13*, 1631. c) S. Liu, J. Zhu, Y. Matsai, I. Felner, A. Gedanken, *Chem. Mater.* **2000**, *12*, 2205. d) L. Sun, P. C. Searson, C. L. Chien, *Appl. Phys. Lett.* **2001**, *79*, 4429.
[3] a) J. P. Pierce, E. W. Plummer, J. Shen, *Appl. Phys. Lett.* **2002**, *81*, 1890. b) Z. Zhang, D. A. Blom, Z. Gai, J. R. Thompson, J. Shen, S. Dai, *J. Am. Chem. Soc.* **2003**, *125*, 7528. c) Y.-G. Guo, L.-J. Wan, C.-F. Zhu, D.-L. Yang, D.-M. Chen, C.-L. Bai, *Chem. Mater.* **2003**, *15*, 664.
[4] a) R. Tenne, L. Margulis, M. Genut, G. Hodes, *Nature* **1992**, *360*, 444. b) L. Margulis, G. Salitra, R. Tenne, *Nature* **1993**, *365*, 113. c) R. Tenne, *Chem. Eur. J.* **2002**, *8*, 5303.
[5] a) M. Nath, C. N. R. Rao, *J. Am. Chem. Soc.* **2001**, *123*, 4841. b) M. Nath, C. N. R. Rao, *Angew. Chem. Int. Ed.* **2002**, *41*, 3451. c) C. N. R. Rao, M. Nath, *J. Chem. Soc. Dalton Trans.* **2003**, 1.
[6] P. Yang, Y. Wu, R. Fan, *J. Nanosci. Nanotechnol.* **2002**, *1*, 1.
[7] a) H. Nakazawa, N. Morimoto, *Mater. Res. Bull.* **1971**, *6*, 345. b) C. N. R. Rao, K. P. R. Pisharody, *Prog. Solid State Chem.* **1976**, *10*, 207. c) J. C. Ward, *Rev. Pure Appl. Chem.* **1970**, *20*, 175.
[8] a) J. L. Horwood, M. G. Townsend, A. H. Webster, *J. Solid State Chem.* **1976**, *17*, 35. b) V. H. Haraldsen, *Z. Anorg. Allg. Chem.* **1937**, *231*, 78. c) E. Hirahara, M. Murakami, *Phys. Chem. Solids* **1958**, *7*, 281.
[9] F. Li, H. F. Franzen, *J. Solid State Chem.* **1996**, *126*, 108.
[10] T. Hirone, S. Maeda, N. Tsuya, *J. Phys. Soc. Jpn.* **1954**, *9*, 736.
[11] a) J. M. D. Coey, H. Roux-Buisson, R. Brusetti, *J. Phys. (Paris)* **1976**, *37*, C4-1. b) M. G. Townsend, J. R. Gosselin, R. J. Tremblay, A. H. Webster, *J. Phys. (Paris)* **1976**, *37*, C4-11. c) J. R. Gosselin, M. G. Townsend, R. J. Tremblay, *Solid State Commun.* **1976**, *19*, 799.
[12] X. Ouyang, T.-Y. Tsai, D.-H. Chen, Q.-J. Huang, W.-H. Cheng, A. Clearfield, *Chem. Commun.* **2003**, 2886.
[13] a) X. Huang, J. Li, *J. Am. Chem. Soc.* **2000**, *122*, 8789. b) Z.-X. Deng, L. Li, Y. Li, *Inorg. Chem.* **2003**, *42*, 2331.
[14] JCPDS (Joint Committee on Powder Diffraction Standards) files-International Center for Diffraction Data **1997**.

Molecular-Scale Interface Engineering of TiO_2 Nanocrystals: Improving the Efficiency and Stability of Dye-Sensitized Solar Cells**

By *Peng Wang*, *Shaik M. Zakeeruddin*,*
Robin Humphry-Baker, *Jacques E. Moser*, and
*Michael Grätzel**

During the last decade, dye-sensitized solar cells (DSCs) have attracted considerable interest as low-cost alternatives to conventional inorganic photovoltaic devices.[1–3] Although an impressive 10 % solar-to-electricity conversion efficiency could be attained with a panchromatic dye, the achievement of long-term stability at temperatures of ~80–85 °C has remained a major challenge for a long time. Very recently, an amphiphilic heteroleptic ruthenium sensitizer referred to as Z-907 (*cis*-$Ru(H_2dcbpy)(dnbpy)(NCS)_2$, where the ligand

[*] Dr. S. M. Zakeeruddin, Prof. M. Grätzel, Dr. P. Wang,
Dr. R. Humphry-Baker, Dr. J. E. Moser
Laboratory for Photonics and Interfaces
Swiss Federal Institute of Technology Lausanne
Lausanne CH-1015 (Switzerland)
E-mail: shaik.zakeer@epfl.ch, michael.graetzel@epfl.ch

[**] The present work is supported by the Swiss Science Foundation, Swiss Federal Office for Energy (OFEN), and the European Office of U.S. Air Force under Contract No. F61775–00-C0003.

 DOI: 10.1002/adma.200306084 © 2003 WILEY-VCH Verlag GmbH & Co. KGaA, Weinheim

ADVANCED MATERIALS

H_2dcbpy is 4,4′-dicarboxylic acid-2,2′-bipyridine and dnbpy is 4,4′-dinonyl-2,2′-bipyridine, Fig. 1) has been developed to fabricate a solar cell with about 6 % efficiency.[4] When combined with a quasi-solid-state polymer gel electrolyte, solar cells resisting thermal degradation have been realized. The introduction of the two hydrophobic alkyl chains on the bipyridyl ligand was critical to pass the thermal stress test.

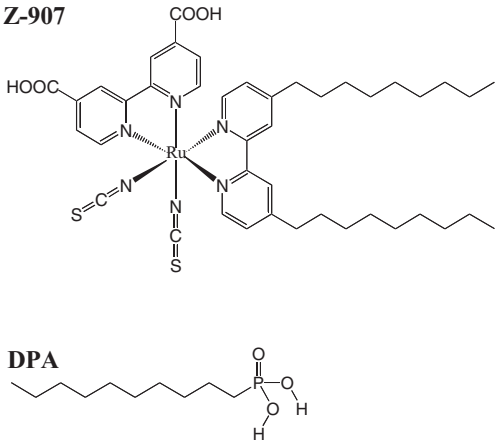

Fig. 1. Molecular structures of Z-907 dye and DPA coadsorbent.

While the overall efficiency remained remarkably stable when these cells were maintained for 1000 h at 80 °C, a drop of the open-circuit photovoltage (V_{oc}) of about 100 mV did still occur over this period, compensated for by a rise in the short-circuit photocurrent (J_{sc}) and the fill factor (ff).[4] Further stabilization of these individual device parameters is warranted for practical reasons. Here we report for the first time on a DSC based on nanocrystalline TiO_2 films that are covered by a mixed self-assembled monolayer of the amphiphilic Z-907 sensitizer and 1-decylphosphonic acid (DPA, Fig. 1). Co-adsorption of DPA is shown to produce a striking stabilization of the voltage output and significant improvement of the conversion efficiency of this photovoltaic device.

The detailed fabrication procedure for the nanocrystalline TiO_2 photoanodes and the assembly of complete, hot-melt sealed cells were described in our previous work.[4] The TiO_2 electrodes were surface derivatized by immersing them into the dye solutions at room temperature for 12 h. Solution **A** consisted of 300 μM Z-907 in acetonitrile and *tert*-butanol (volume ratio: 1:1), and solution **B** contained 300 μM Z-907 dye and 75 μM DPA as co-adsorbent. The new electrolyte contained 0.6 M 1-propyl-3-methylimidazolium iodide, 0.5 M *N*-methyl-benzimidazole, and 0.1 M I_2 in 3-methoxypropionitrile. The cells without and with DPA co-adsorbent are denoted as device **A** and **B**, respectively.

Figure 2 shows attenuated total reflection Fourier-transform infrared (ATR-FTIR) spectra of a mesoporous TiO_2 film derivatized with Z-907 alone and with a mixed monolayer of Z-907 and DPA. Spectrum (a) was obtained from films stained by solution **A** containing only the Z-907 sensitizer. The single feature at 2101 cm^{-1} arises from the thiocyanato

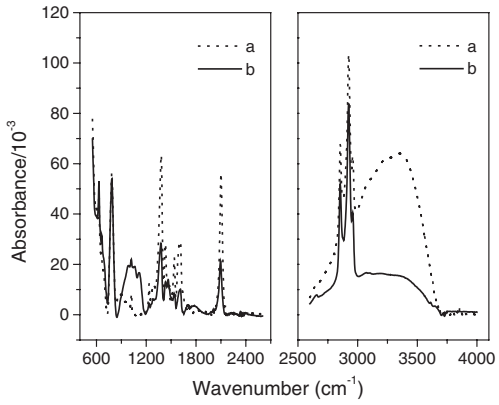

Fig. 2. ATR-FTIR spectra for 4 μm mesoporous TiO_2 film coated with a) only Z-907 dye and b) Z-907 dye and DPA coadsorbent. In the left panel a TiO_2 reference film heated at 500 °C to remove surface-adsorbed water has been subtracted for clarity of presentation.

group, the signals at 1607 and 1379 cm^{-1} are due to the symmetric and asymmetric stretching modes of carboxylate groups, and the peaks observed at 2925 and 2855 cm^{-1} correspond to the asymmetric and symmetric stretching modes of the CH_2-units of the aliphatic chains. The sharp peaks located at 1537, 1429, 1236, and 1019 cm^{-1} arise to bipyridyl modes while the large and broad feature at 3370 cm^{-1} is due to adsorbed water.

If the film is stained from solution **B** containing both Z-907 and DPA, co-grafting of the two amphiphiles is confirmed by the appearance of the P–O stretching bands[5] at 1057 and 1120 cm^{-1}. The FTIR signal from surface adsorbed water is suppressed by DPA co-adsorption, indicating that access of water to the surface of the anatase nanocrystals is much more restricted in the case of the mixed monolayer than for the amphiphilic Z-907 dye alone. Alkylphosphonic acids are known to strongly bind to oxide surfaces through formation of P–O–metal bonds,[5–8] eliminating most of hydrophilic surface sites that remain available for water adsorption even after grafting of the Z-907 dye.

Although the molar ratio of Z-907 to DPA in dye solution is only 4:1, the surface concentration of the sensitizer is reduced by 30 to 40 % in the presence of DPA, as determined by optical absorption experiments with transparent nanocrystalline films of about 4 μm thickness. This is due to the fact that DPA has a higher affinity to interact with the TiO_2 than Z-907. Photo-acoustic FTIR experiments show that dye and DPA are evenly distributed across the whole depth of the nanocrystalline TiO_2 film.

Figure 3a presents the photocurrent–voltage curves measured in full air mass 1.5 sunlight (intensity of the solar simulator 100 mW cm^{-2}, spectral mismatch corrected), and Table 1 lists the overall conversion efficiencies at different light intensities. The J_{sc}, V_{oc}, and *ff* of device **A** are 13.6 mA cm^{-2}, 721 mV, and 0.692, respectively, yielding an overall conversion efficiency (η) of 6.8 %. The corresponding parameters (J_{sc}, V_{oc}, *ff*, and η) of device **B** are 14.6 mA cm^{-2}, 722 mV, 0.693, and 7.3 %, respectively. Thus, the TiO_2 film derivatized

 © 2003 WILEY-VCH Verlag GmbH & Co. KGaA, Weinheim

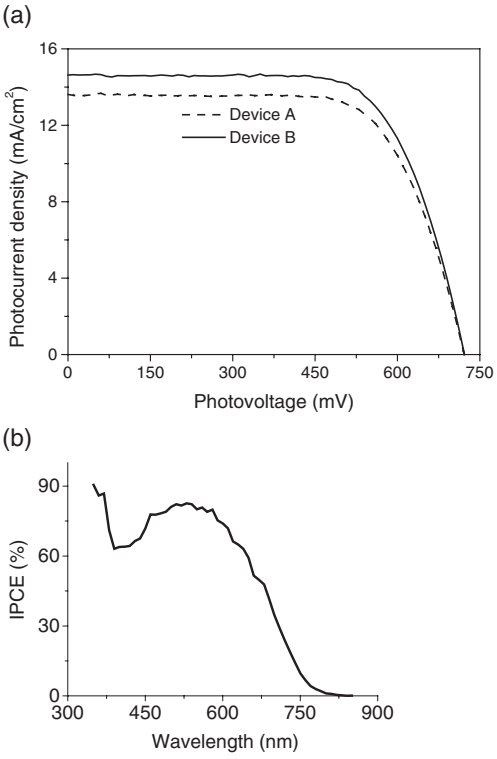

Fig. 3. a) Photocurrent density–voltage characteristics of device **A** and **B** at air mass 1.5 (100 mW cm^{-2}) illumination. b) The IPCE spectrum for device **B**. Cell active area: 0.152 cm^2.

Table 1. Device efficiencies of DSCs under various sunlight irradiation intensities.

Device	η [%] at different light intensities [a]		
	0.1 Sun	0.5 Sun	1.0 Sun
A	7.6	7.4	6.8
B	7.8	7.7	7.3

[a] The spectral distribution of the lamp mimics air mass 1.5 solar light. 1.0 Sun corresponds to an intensity of 100 mW cm^{-2}.

with the mixed monolayer delivers a higher photocurrent than the film containing Z-907 dye alone. As the two systems give very similar fill factors and photovoltages the overall conversion efficiency for device **B** is superior to that of **A**.

The photocurrent action spectrum of device **B** is shown in Figure 3b. The maximum incident photon-to-current conversion efficiency (IPCE) value is 83 % at 540 nm and close to 40 % at 700 nm. This shows that any reduction of the light harvesting by the Z-907 dye due to the dilution with the co-grafted 1-decylphosphonate must be compensated by a gain in the quantum yield of electron injection or a smaller recombination loss during the electron percolation across the nanocrystalline TiO_2 film.

Importantly, photoanodes based on TiO_2 nanocrystals derivatized by Z-907 and DPA were found to maintain a strikingly stable performance under thermal stress and long term light soaking. As shown in Figure 4a, the V_{oc} of such a device drops only by 20 mV, i.e., less than 3 %, during 1000 h aging at 80 °C while films derivatized with the Z-907 sensitizer alone

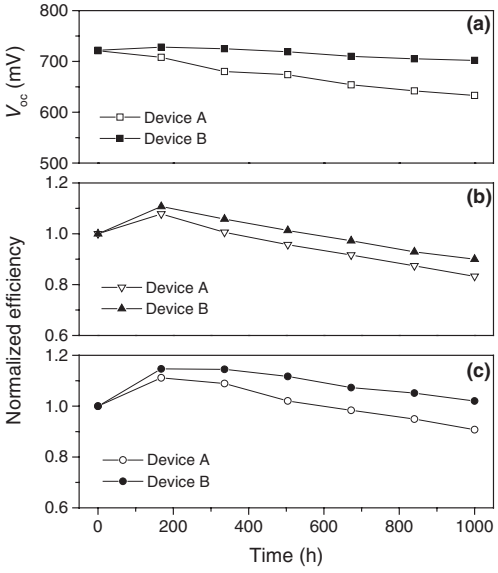

Fig. 4. a) Open-circuit photovoltages, b) normalized device efficiencies during accelerated aging at 80 °C, and c) normalized device efficiencies during successive one sun visible-light soaking at 55 °C.

show a decline of 90 mV. The voltage stability exhibited by the DPA/Z-907 mixed monolayer based cells is unprecedented for DSCs, which are notorious for showing a rather large decline in the V_{oc} value when monitored at 80 °C.[9] A likely reason for the stabilizing effect of the long-chain phosphonate on the photovoltage is the exclusion of water from the interface. The role of surface water is presently being further investigated. This stabilization of the V_{oc} allows the high conversion efficiency of device **B** to be sustained during extended heat exposure. Figure 4b shows that this device maintained over 90 % of its initial conversion yield after 1000 h aging at 80 °C. This is the first time that DSCs having >7 % efficiencies passes this test, which is very important for practical use of these solar cells.

The device also showed an excellent photostability when submitted to accelerated testing in a solar simulator at 100 mW cm^{-2} intensity. Thus, the efficiency showed no drop after 1000 h of light soaking at 55 °C (Fig. 4c). The cell was covered with an ultraviolet (UV)-absorbing polymer film. Applying the UV filter reduced the overall efficiency only slightly from 7.3 to 7.1 %, i.e., by ca. 3 %.

In conclusion, we have demonstrated that the use of mixed self-assembled monolayers containing a hydrophobic phosphonate apart from the amphiphilic ruthenium sensitizer enhances the efficiency and stability of dye-sensitized solar cells. For the first time, long-term thermally stable devices with higher than 7 % power conversion efficiency have been fabricated and the photovoltage drop of the DSC under heat stress has been greatly attenuated. The extraordinary stability of this high-efficiency device under both thermal stress and light soaking matches the durability criteria for outdoor applications of solar cells.

Received: August 28, 2003

 © 2003 WILEY-VCH Verlag GmbH & Co. KGaA, Weinheim

ADVANCED MATERIALS

[1] B. O'Regan, M. Grätzel, *Nature* **1991**, *353*, 737.
[2] A. Hagfeldt, M. Grätzel, *Acc. Chem. Res.* **2000**, *33*, 269.
[3] M. Grätzel, *Nature* **2001**, *414*, 338.
[4] P. Wang, S. M. Zakeeruddin, J. E. Moser, M. K. Nazeeruddin, T. Sekiguchi, M. Grätzel, *Nat. Mater.* **2003**, *2*, 402.
[5] E. S. Gawalt, G. Lu, S. L. Bernasek, J. Schwartz, *Langmuir* **1999**, *15*, 8929.
[6] J. T. Woodward, D. K. Schwartz, *J. Am. Chem. Soc.* **1996**, *118*, 7861.
[7] S. Pawsey, M. McCormick, S. De Paul, R. Graf, Y. S. Lee, L. Reven, H. W. Spiess, *J. Am. Chem. Soc.* **2003**, *125*, 4174.
[8] R. Hofer, M. Textor, N. D. Spencer, *Langmuir* **2001**, *17*, 4014.
[9] A. Hinsch, J. M. Kroon, R. Kern, I. Uhlendorf, J. Holzbock, A. Meyer, J. Ferber, *Prog. Photovoltaics* **2001**, *9*, 425.

A Single Photochromic Molecular Switch with Four Optical Outputs Probing Four Inputs**

By *He Tian*,* *Bing Qin*, *Rongxia Yao*, *Xueli Zhao*, and *Songjie Yang*

Many researchers have considered how to exploit molecular properties, with their intrinsic diversity, to create molecular switches. The use of photochromic compounds, such as spiropyran and diarylethene, as photoswitching systems attracts much attention because of their potential ability for application in photonic devices, where each isomer of the photochromic compound can represent "0" or "1" of a digital binary code.[1] Raymo and Giordani[2] demonstrated the modulation of pyrene fluorescence in the presence of spiropyran under three external inputs (ultraviolet (UV) and visible (vis) light and protons) by taking advantage of the different absorption properties of three states of spiropyran, which was proposed for use in multichannel signal communication. Zhu and coworkers proposed a new molecular logic circuit based on the fact that the excimer fluorescence of bis-pyrene can be reversibly regulated by UV light, metal ions, and visible light in the presence of spiropyran.[3] However, these multi-channel signal communication systems relied on two molecules per system. In fact, one key aspect sought in the progress of molecular switching technology is the development of smarter systems that integrate several switchable functions into a single molecule.[4–6]

1,2-Bis(thienyl)ethene derivatives (BTEs)–metalloporphyrin switches, in which the transition metal is coordinated to the ends of the pyridyl-derived BTE, were suggested to achieve non-destructive readout using phosphorescence instead of fluorescence changes.[6a,b] The interaction between the metal ions located at both ends of the pyridyl groups of the diarylethene can be switched by irradiation, because the π-conjugated bond structures between the two aryl groups in the two isomers are different.[7,8] On the other hand, reversible changes of luminescence of BTEs are interesting from the viewpoint of applications for erasable memory media, optical switches, and fluorescence probes. Irie et al.[9] have shown that digital switching of the fluorescence of diarylethene molecules can be controlled by irradiation with UV/vis light at the single-molecule level. Based on the changes of near-infrared (IR) luminescence along with photochromism, a novel family of photochromic BTE-based tetraazaporphyrin or phthalocyanine hybrids was developed in our lab as excellent, non-destructive readout media for application in optical switches.[10]

In this communication, a photochromic pyridine-tethered BTE (Py-BTE), namely bis(5-pyridyl-2-methylthien-3-yl)cyclopentene (see Scheme 1),[11a] is used as a photoswitch responding to metal ions, protons, and alternating UV/vis light irradiation. The compound Py-BTE has a special selective response to Zn^{2+} and is also very sensitive to protons. The fluorescent properties, including the intensity and emission peak wavelengths of the compound, can be reversibly regulated by UV-vis light, Zn^{2+}, and protons. Based on these results, a complicated molecular switch is proposed. To the best of our knowledge, it is the first time that only one photochromic compound is used to build a molecular switch with four optical outputs responding to four inputs.

Upon irradiation with light of 254 nm, the colorless open-ring form Py-BTE becomes purple ($\lambda = 558$ nm), which is due to the transformation of Py-BTE by photocyclization into its closed form (**1c**).[11a] Py-BTE can be photochemically regenerated from its closed form by irradiation with light of 570 nm, and the characteristic purple color of the closed form disappears. Similar photochromism was observed for (Py-BTE)Zn in tetrahydrofuran (THF) under identical conditions, as shown in Scheme 1.

There are two conformations of BTE, which are in dynamic equilibrium, with the two rings in mirror symmetry and in C_2 symmetry; however, only the anti-parallel conformation can participate in the photocyclization reaction. Therefore, only the ratio of the anti-parallel conformation increases, and thus the photocyclization quantum yield can be expected to increase.[1] It is worthwhile to note that the photochromism is enhanced three times for (Py-BTE)Zn. The ring-closure coloration quantum yield increases from 15.5 % (for Py-BTE alone) to 44.6 % upon the addition of various amounts of Zn^{2+}. Zinc ions may form a favorable configuration complex with Py-BTE, which may favor the anti-parallel conformation of BTE.[11a] No enhancement of the photochromism was observed for other metal ions, including Cu^{2+}, Ni^{2+}, Co^{2+}, and Mn^{2+} in the same system,[12] which means that the compound Py-BTE has a special selective response to Zn^{2+}.

Recording the change of luminescence in order to process stored information can minimize the extent of erased information during detection; however, another important condition must be met additionally. That is, the emission wave-

[*] Prof. H. Tian, B. Qin, R. Yao, X. Zhao, Dr. S. Yang
Institute of Fine Chemicals
East China University of Science and Technology
Shanghai 200237 (P.R. China)
E-mail: tianhe@ecust.edu.cn

[**] H. T. acknowledges support by the NSFC/China, Education Committee of Shanghai, and Scientific Committee of Shanghai. The authors greatly appreciate Prof. A. Prasanna de Silva (Queen's University) and the referees for their helpful and valuable comments—some sentences in the discussion originate from their comments and suggestions. Supporting information for this article is available online or from the author.

 © 2003 WILEY-VCH Verlag GmbH & Co. KGaA, Weinheim **DOI:** 10.1002/adma.200305425 *Adv. Mater.* **2003**, *15*, No. 24, December 17